AD_____

Award Number: DAMD17-03-1-0342

TITLE: Elucidation of Prion Protein Conformational Changes
Associated with Infectivity by Fluorescence Spectroscopy

PRINCIPAL INVESTIGATOR: Michele A. McGuirl, Ph.D.

CONTRACTING ORGANIZATION: University of Montana
Missoula, MT 59812-1825

REPORT DATE: June 2005

TYPE OF REPORT: Annual

PREPARED FOR: U.S. Army Medical Research and Materiel Command
Fort Detrick, Maryland 21702-5012

20060503281

REPORT DOCUMENTATION PAGE

Form Approved
OMB No. 0704-0188

Public reporting burden for this collection of information is estimated to average 1 hour per response, including the time for reviewing instructions, searching existing data sources, gathering and maintaining the data needed, and completing and reviewing this collection of information. Send comments regarding this burden estimate or any other aspect of this collection of information, including suggestions for reducing this burden to Department of Defense, Washington Headquarters Services, Directorate for Information Operations and Reports (0704-0188), 1215 Jefferson Davis Highway, Suite 1204, Arlington, VA 22202-4302. Respondents should be aware that notwithstanding any other provision of law, no person shall be subject to any penalty for failing to comply with a collection of information if it does not display a currently valid OMB control number. **PLEASE DO NOT RETURN YOUR FORM TO THE ABOVE ADDRESS.**

1. REPORT DATE *(DD-MM-YYYY)* 01-06-2005	2. REPORT TYPE Annual	3. DATES COVERED *(From - To)* 15 May 2004 – 14 May 2005

4. TITLE AND SUBTITLE Elucidation of Prion Protein Conformational Changes Associated with Infectivity by Fluorescence Spectroscopy	5a. CONTRACT NUMBER
	5b. GRANT NUMBER DAMD17-03-1-0342
	5c. PROGRAM ELEMENT NUMBER
6. AUTHOR(S) Michele A. McGuirl, Ph.D. E-Mail: Michele.mcguirl@umontana.edu	5d. PROJECT NUMBER
	5e. TASK NUMBER
	5f. WORK UNIT NUMBER

7. PERFORMING ORGANIZATION NAME(S) AND ADDRESS(ES) University of Montana Missoula, MT 59812-1825	8. PERFORMING ORGANIZATION REPORT NUMBER

9. SPONSORING / MONITORING AGENCY NAME(S) AND ADDRESS(ES) U.S. Army Medical Research and Materiel Command Fort Detrick, Maryland 21702-5012	10. SPONSOR/MONITOR'S ACRONYM(S)
	11. SPONSOR/MONITOR'S REPORT NUMBER(S)

12. DISTRIBUTION / AVAILABILITY STATEMENT
Approved for Public Release; Distribution Unlimited

13. SUPPLEMENTARY NOTES

14. ABSTRACT
Prion diseases are fatal neurodegenerative diseases of mammals. They are characterized by the conversion of normal prion protein (PrP) to a misfolded conformational state that accumulates as plaques in the brain. The diagnosis of prion diseases relies on the ability to differentiate between normal PrP and its misfolded, infectious form. This is difficult to accomplish by traditional testing methods, since it requires discerning between conformational states of a protein that is present in both normal and diseased tissue, rather than identifying the appearance of a new protein associated with infection. We wish to design a reporter PrP substrate that may be monitored by fluorescence spectroscopy. After the conversion of normal-PrP to its infectious state, some amino acid residues of PrP will undergo a change in their local solvent environment. We propose to identify these residues by monitoring the fluorescence emission spectrum of a series of mutant 7-AzaTrp-substituted PrP proteins. The 7-AzaTrp fluorescence emission spectrum is both unique compared with normal Trp and exquisitely sensitive to its local environment. This could lead to the development of a rapid, sensitive, and inexpensive technique to detect infectious PrP, based on its ability to bind 7-AzaTrp-substituted PrP, and convert it to the misfolded form.

15. SUBJECT TERMS
Prion fluorescence assay structure 7-azatryptophan

16. SECURITY CLASSIFICATION OF:			17. LIMITATION OF ABSTRACT	18. NUMBER OF PAGES	19a. NAME OF RESPONSIBLE PERSON
a. REPORT U	b. ABSTRACT U	c. THIS PAGE U	UU	18	19b. TELEPHONE NUMBER *(include area code)*

Standard Form 298 (Rev. 8-98)
Prescribed by ANSI Std. Z39.18

Table of Contents

INTRODUCTION

Prion diseases are fatal neurodegenerative diseases of mammals and include Creutzfeld-Jacob disease (humans), scrapie (sheep), chronic wasting disease (elk, deer), and mad cow disease (cattle).[1] The diseases are characterized by the conversion of normal prion protein (PrP) to a misfolded conformational state that aggregates and forms plaques in the brain. Although this conversion process is poorly understood, it is known that the aggregate-prone form has a higher β-sheet content than does normal PrP. To differentiate between normal PrP and its misfolded, infectious form and assist in diagnosis of the diseased state, we wish to design a reporter PrP substrate peptide that will exhibit unique fluorescent properties upon contact with infectious PrP and/or its subsequent conversion. The sequence of the reporter peptide will be based upon experiments conducted with recombinant PrP. We will identify individual PrP residues that undergo changes in their local solvent environment upon conversion by measuring the fluorescence emission spectra of a series of mutant 7-AzaTrp-substituted PrP proteins. The 7-AzaTrp absorbance spectrum is red-shifted compared with Trp, and its fluorescence emission spectrum is exquisitely sensitive to its local environment.[2] Therefore, the conversion of the analog-substituted PrP substrate will be easily detected against a background of Trp-containing protein aggregates.

BODY

Overview

In this past year we have nearly finished *Task 1* and have made progress on *Task 2.* Dr. Hui-Chun Yeh, a post-doctoral scholar, left the laboratory in January 2005 to join her fiancé in Texas. During the seven months prior to her departure, Dr. Yeh (assisted by Ms. Erin Gray, a part time technician) produced, purified, and characterized five new PrP mutants and investigated their biophysical properties. Dr. Yeh is currently working on a manuscript based on this work. Ms. Gray refined the process of analog incorporation into PrP (*Task 2a*). We are now routinely achieving ~85% analog incorporation into PrP mutants, which is sufficient for us to finish the aims of *Task 2*. Ms. Gray is now pursuing graduate studies in neuroscience at UCLA. The departures of these staff members have hampered the progress of the work this year. This spring, I began to train Ms. Yanchao Ran, a first year graduate student who has decided to join my laboratory. Ms. Ran worked closely with Ms. Gray and is now ready to continue the project. In addition, I have hired Mr. Rong Wang to work on the project for the next few months. Mr. Wang will receive his PhD this summer and is available for the next 4-6 months, before he begins his postdoctoral studies at Rocky Mountain Laboratories/NIAID. Mr. Wang is an outstanding scientist who is pursuing *Task 1e.* We have also begun a collaboration with Dr. Valerie Daggett of the University of Washington. Dr. Daggett has produced a model of β-PrP using molecular dynamics simulations.(3) We firmly believe that our fluorescence data will discern whether her model, or that put forth by Govaerts et al (4) is a more accurate depiction of the structure of β-PrP.

Accomplishments related to Task 1. Identify surface residues of the normal PrP form that change conformation and/or participate in binding to aggregated PrP. (Months 1-24)

1a) Express a series of Trp-substituted mutants of truncated Syrian hamster PrP (90-231) in E. coli.

Expression: We have expressed truncated Syrian golden hamster PrP (residues 90-231) in *E. coli*, as outlined in the Methods Section of our proposal. We continue to use the robust pET expression vector and the Rosetta cell strain (Novagen) for expression, since it is proven to work for full-length PrP. (5) By using the commercially available Rosetta cell strain from Novagen, we have increased the expression levels of both full-length and truncated PrP to nearly 30 mg/liter of culture.

Mutants Produced: This year we have produced and characterized five single Trp PrP mutants, bringing the total variants available for study up to nine (see Table I). New mutants include two from the original list (S135W, Y218W), two that were added last year and given high priority mutants (Y150W, Y163W), and a new mutant (L125W) that was suggested by discussions with Dr. Valerie Daggett. Dr. Daggett of the University of Washington. Dr. Daggett and Mari DeMarco, her talented graduate student, have made a model of β-PrP using molecular dynamics simulation.(3) This enables us to predict changes in solvent accessibility and local environment that occur upon conversion. This model is referred to as the β-spiral form. In addition, we have secured the coordinates to the Govaerts model of β-PrP, termed the β-helix model (4) - the coordinates for neither β-PrP model have been publicly released. Comparing these two models with the α-PrP structure (6) has significantly re-shaped our priority list of mutants. Table 1 summarizes our finalized list of mutants.

Table I. PrP Mutants: Bold blue font, made and characterized as of 5/14/05; italicized red font, new proposed mutants based on the newly available models of β-PrP; normal font, mutants that were originally proposed that now have low priority.

Trp Mutant	Region of Interest	Rationale for Choice
Wild Type residues 90-231		Control protein for comparison with mutants and with data published by others
Trp99Phe	H1 143-156	Examine Trp fluorescence from W145 in H1
Trp145Tyr	90-120	Examine Trp fluorescence from W99, in conformationally dynamic region (structurally undefined)
W99F/W145Y	Trp-free Base mutant	Remove Trp fluorescence from control protein, Use this for the other mutations listed below
Tyr218Trp W99F/W145Y	200-223	Internal residue in H3 near disulfide bond, contacts H2
Tyr150Trp W99F/W145Y	H1 143-156	Internal residue in H1; suggested to become solvent exposed after conversion(3)
Tyr163Trp W99F/W145Y	158-165	Partially exposed residue in loop near H2 and H3 suggested to become more solvent exposed after conversion(3)
Ser135Trp W99F/W145Y	119-136	Surface residue in coil region
Leu125Trp W99F/W145Y	unstructured	Predicted to be solvent exposed in α-PrP and β-spiral, buried in β-helix.
Gly123Trp W99F/W145Y	unstructured	Predicted to be solvent exposed in α-PrP and β-spiral, buried in β-helix.
Asp144Trp W99F/W145Y	H1 143-156	Predicted to be solvent exposed in α-PrP and β-spiral, buried in β-helix.
Asn159Trp W99F/W145Y	158-165	Predicted to be buried in α-PrP and β-spiral, solvent exposed in β-helix.
Lys106Trp W99F/W145Y	90-120	In conformationally dynamic region (structurally undefined)
Asn108Trp W99F/W145Y	90-120	In conformationally dynamic region (structurally undefined)
Met134Trp W99F/W145Y	119-136	Internal residue in coil region, contacts H3
Asn170Trp W99F/W145Y	166-179	Surface residue in loop near H2 and H3
His177Trp W99F/W145Y	166-179	Surface residue in H2
Gln212Trp W99F/W145Y	200-223	Surface residue in H3
Lys220Trp W99F/W145Y	200-223	Surface residue in H3

Purification: We have purified nine mutants to homogeneity using the protocol outlined in the previous report. Typical yields are 10 mg purified PrP per liter of culture.

Tasks 1 (b-d) For each mutant: (b) determine the stability of the α-structure by CD (circular dichroism) temperature unfolding experiments; (c) determine the solvent exposure of the introduced Trp residue by fluorescence spectroscopy; and (d) determine if conversion to a soluble β-structure changes the solvent exposure by fluorescence spectroscopy.

Determination of the concentrations of PrP variants: The protein concentration of PrP variants is routinely determined using the Bradford Dye Assay (Biorad, BSA standard). Our studies indicate no differences in the dye response of β-PrP compared with α-PrP. However, the dye assay introduces an inherent error in using BSA as a standard for PrP – the standard may have a different affinity for the dye than PrP. Therefore, we have determined the ε_{280} molar extinction coefficient for mutants in the α-form by magnetic circular dichroism, MCD (7,8); we plan to extend these studies to all mutants and to their β-forms. MCD accurately measures the Trp content of a sample – the Trp MCD signal is an intrinsic property of the indole side chain and is not influenced by protein or solvent micro-environments. Once the Trp content was determined by MCD (Figure 1), the UV absorbance was measured and an extinction coefficient was calculated from the experimental data (Table 2).

Figure 1. MCD spectra of ~ 1 mg/mL PrP wt and two mutants (90-231), showing the signal at 292 nm due to tryptophan. The data were collected at field strength of 0.738 T. Calibration was done with potassium ferricyanide at 23C. The data were used in conjunction with UV absorbance measurements to determine the molar extinction coefficients (Table 2) at 280 nm for each mutant.
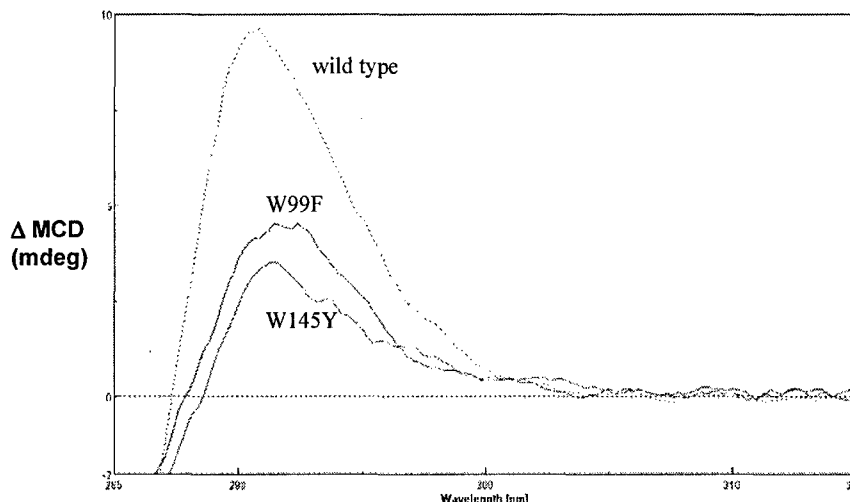
Table 2. Extinction coefficients of PrP Mutants.

| MCD Sample	#Trp per protein	ε_{280} $(M^{-1}cm^{-1})$
Lysozyme standard	6 (expt'l = 5.98)	---
PrP wild type 90-231	2	23,510
PrP W145Y	1	19,550
PrP W99F	1	20,470

Conversion Method: We routinely convert α-PrP to the β-form by using a modification of the method described by Baskakov et al. (9) α-PrP is first unfolded in 20 mM Na-Acetate, 0.2M NaCl, pH 3.7 + 10M Urea. The sample is then diluted to 5M urea in the same buffer and incubated at 27C for 48 hours. Afterwards, the urea is removed by dialysis into urea-free buffer (pH 5.5) at 4°C. Using this method, PrP is converted with ~100% efficiency and is stable for weeks.

Spectroscopic Techniques: The thermal denaturation profile of each mutant was measured, to assess the effects of mutation on the overall structural stability of the α-form. The thermal unfolding was monitored by Circular Dichroism spectroscopy (CD) and the melting temperature (T_M) was determined at 222 nm. The CD instrument is a Jasco 810 fitted with a peltier cell holder and scanning fluorescence detector. All mutants examined thus far exhibit only minor deviation from simple two-state unfolding and have similar T_M values (ranges 62- 68 C), indicating that the mutations do not affect global stability. The data are consistent with the

7

published T_M for full-length PrP. (10) For comparative experiments of α- and β-PrP by CD and fluorescence, samples were run in 20 mM Na-Acetate, 0.2 M NaCl, pH 5.5 at 25°C. The protein concentration was ~50 µM; Note that a 1 mM path length was used for CD; alternatively the samples were diluted 10-fold and the spectra recorded in a 1 cm pathlength cuvette. CD data were processed to determine the MRE (mean residue ellipticity) units, to ensure that full conversion had taken place. Fluorescence data were normalized for differences in protein concentration. CD and MCD measurements were collected using 1 nm data pitch, 200 nm/min scan speed, 2 nm band width, 1 sec response. Thermal denaturation curves were determined every 5° from 20 – 90°C at 222 nm (α-helix peak) using a temperature slope of 2°C/minute.

Figure 2. Characterization of µM wild type PrP in α (blue/solid) and β (green/dashed) forms. (a) CD spectra; (b) Trp fluorescence.
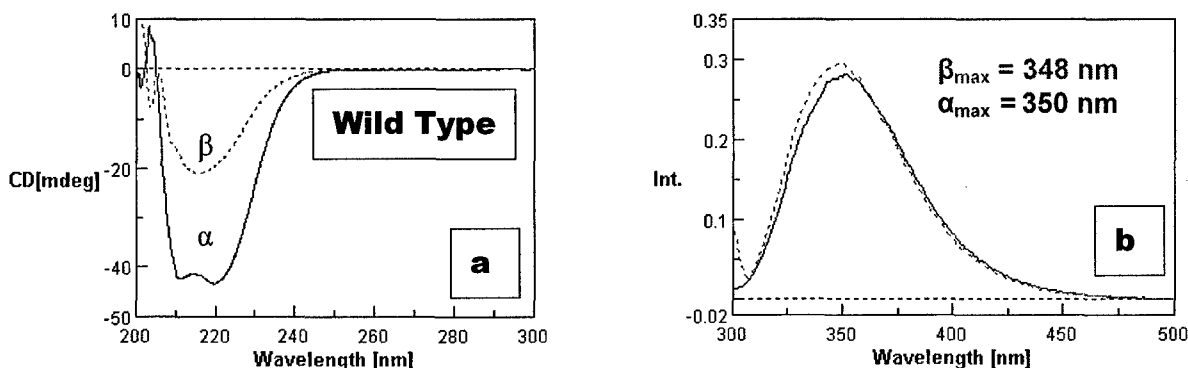
The conversion process has also been confirmed by CD spectroscopy, which detects changes in the α-helical content of proteins. A typical result is shown in Figure 2a. The monomeric α-helical form displays a CD spectrum with two negative peaks; the bands at 222 and 210 nm indicate a large α-helical content.(4) Upon conversion, there is a dramatic change in the CD spectrum. Converted β-PrP displays a single negative band of ~ 50% the intensity, with λ_{max} at 218 nm.

The fluorescence emission spectra of the α- and β-forms of each PrP variant were measured after excitation at 295 nm (conditions: 2 or 5 nm bandwidth, 1 nm data pitch, 0.25 sec response, 1 cm path length cuvette). The data for each mutant are summarized in Table 3. In general, blue-shifted bands (< 340 nm) indicate that Trp is in a hydrophobic pocket, whereas peak maxima near 355 nm suggest that Trp is in a highly solvated, exposed environment. It should be noted that both the quantum yield and wavelength maximum of Trp fluorescence also depends on local polarization effects caused by water (solvent) and protein dipoles.(11,12) Representative spectra are shown in Figure 3 (L125W mutant).

Figure 3. Characterization of L125W PrP (also W99F/W145Y) in α (blue/solid) and β (green/dashed) forms. (a) CD spectra; (b) Trp fluorescence.
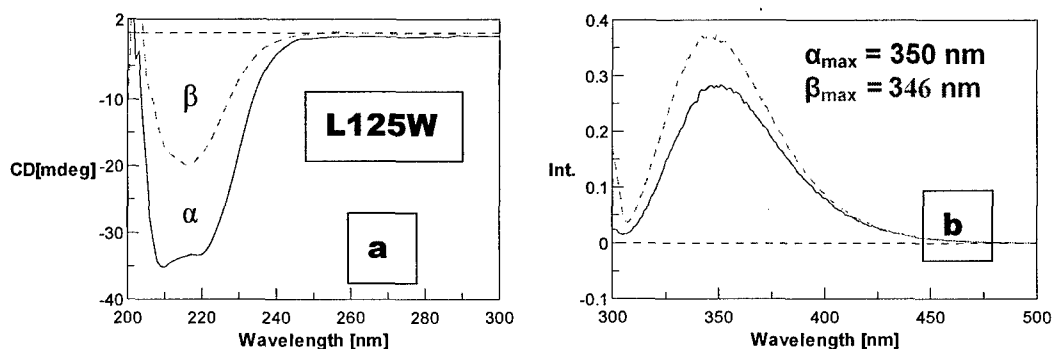
Protein	α-PrP (λ max, Signal Intensity)		β-PrP (λ max, Signal Intensity)	
Wt (W99, W145)	350	0.3047	348	0.3347
W99 (W145Y)	351	0.2029	350	0.1346
L125W (W99F/W145Y)	350	0.2780	346	0.3716
S135W (W99F/W145Y)	350	0.5684	345	0.4321
W145 (W99F)	349	0.2272	347	0.2677
Y150W (W99F/W145Y)	337	0.6667	343	0.3249
Y163W (W99F/W145Y)	341	0.1664	346	0.2575
Y218W (W99F/W145Y)	342	0.1286	346	0.2967

The data indicate that several of the mutants are excellent reporters of the structural changes that occur upon conversion of α-PrP to the β-form. In particular, Y150W undergoes a dramatic 7-nm red-shift in λmax, accompanied by about a 50% quench in fluorescence. This is generally associated with an increase in solvent accessibility. Y163W and Y218W also red-shift in fluorescence maxima, however, these mutants show an increase in fluorescence intensity. L125W and S135W undergo 5-6 nm blue-shifts; the intensity of L125W increases by about 36%, whereas S135W displays a 24% decrease.

The availability of the coordinates for two distinct models for β-PrP makes it possible to do detailed computational analyses of the Trp fluorescence data. This will be done with the guidance of Dr. Patrik Callis from Montana State University/Bozeman. Dr. Callis is a world-renowned expert in the theory and computational analysis of Trp fluorescence. (11,12) We plan to interpret the fluorescence spectra of α-PrP in relation with its NMR structure, and to then do the same for the two β-PrP models. See the Appendices for structural details of the models.

The evaluation of the β-PrP models should discern which is better supported by the results of our solution spectroscopy, and perhaps will lead to a refinement of the better model. This cannot be done by a cursory glance at the structures. For example. Y150 is found within the protein core in the NMR structure of α-PrP, stacked over Ile205. Its phenol group is hydrogen-bonded to Asp202. In the β-spiral model, Y150 is not significantly displaced, but the protonation of Asp202 in this acidic form precludes H-bond formation. This may account for the observed changes in fluorescence upon conversion. In the β-helix model, Y150 is located on the surface of the protein, but it lies at the subunit interface. His110 of another subunit lies close to Y150, as does Arg148 of the same subunit. Since His and Arg is known to efficiently quench Trp fluorescence,(13) this is also a reasonable explanation for the observed quench in fluorescence in Y150W. Only a detailed computational analysis will provide sufficient data for validation of one β-model over another.

We would like to more thoroughly characterize the aggregated β-forms produced by our conversion method. To this end, we have recently purchased an Asymmetric Flow Field Flow Instument (AF$_4$) from PostNova (university funds). This method will permit us to assess the dimensions and oligomeric state(s) of converted PrP. Moreover, we will be able to follow the

thermodynamics and kinetics of β-PrP binding to the reporter proteins we produce for *Task 2*. AF₄ is cutting-edge technology and we look forward to the delivery of this new instrument.

Task 1e. For each mutant, determine if copper or manganese binding influences fluorescent spectrum of either the soluble α-form or soluble β-form.

The departure of Dr. Yeh prevented us from accomplishing this task. The "soon-to-be-Dr." Rong Wang is actively pursuing these experiments.

Accomplishments related to Task 2. Create a 7-AzaTrp-substituted PrP protein as a reporter protein that may be used to detect infectious PrP in the field. (Months 25-36)

Although the Statement of Work indicates that these experiments will be done in Year 3, we began working on this project in earnest in Year 2. 7-azaTrp has a red-shifted absorption spectrum compared with Trp (see Figure 4). Excitation at 310 nm allows 7-AzaTrp to be selectively excited, with little to no contribution from natural amino acids. Moreover, 7-AzaTrp is exquisitely sensitive to its local solvent environment and exhibits long lifetimes.(2)

2a) Based on the results of Task 1, one or more Trp-substituted sequence positions of the truncated PrP will be expressed in a Trp auxotroph strain of *E. coli*, to incorporate 7-aza-tryptophan in lieu of the normal amino acid.

The yield of Trp analog incorporation into recombinant proteins depends on the use of Trp-auxotrophic *E. coli* strains. We expressed wild type truncated PrP using the pET expression vector and CT19(DE3) cells (genotype *aspC, ilvE, tyrB, avtA, trpB*; auxotrophic for Asp, Ile, Leu,Phe, Tyr, and Trp, provided by DS Waugh). The pRARE plasmid from Novagen was also included, to eliminate codon bias. In the previous report, we gre cells to OD₆₀₀ = 2.0 in media containing CAS amino acids supplemented with 50 mg/L L-tryptophan. Protein expression levels were much lower than for the normal BL21(DE3) host strain – only ~ 2 mg/L of culture. After purification, a trypsin digest of the protein was analyzed by electrospray mass spectrometry. The results indicated a 50/50 mixture of normal peptides and analog-substituted peptides. (7-AzaTrp is +2 mass units larger than Trp at acidic pH). The analog was evenly distributed between the W99 and W145 tryptic peptides.

In Year 2 Ms. Erin Gray worked to increase the yields of both expression and analog incorporation. She cloned the *prp* coding sequence for residues 90-231 into pTrcHis, a vector that uses a *trc*-based promoter (trp-lac hybrid). Unfortunately, PrP was not expressed in this vector, regardless of the *E. coli* host strain used. This was similar to the results we previously reported when the pQE vector was used. Rather than continue to subclone *prp* into different vectors, Ms. Gray chose instead to optimize analog incorporation in the existing pET system. By manipulating the growth media prior to induction and changing the growth conditions, we now achieve 85-90% incorporation of 7-azaTrp into PrP mutants (Table 4), as determined by mass spectrometry. Analog incorporation did not alter the midpoint (Tm) or the shape of the CD melting curves for the α-PrP mutants.

Table 4. AzaTrp incorporation into PrP.

PrP mutant	% Analog Incorporation	Tm
Wild Type (old method)	50% (old method)	63.7
W99 (W145Y)	90%	65.2
W145 (W99F)	90%	64.1
Y163W (W99F/W145Y)	90%	63.0
Y218W (W99F/W145Y)	85%	64.7

2b-d) The fluorescence spectrum of this substrate protein will be determined in its soluble α- and β-forms. The substrate protein will be exposed to an aggregated, insoluble β-form of PrP (PrP-res) produced by *in vitro* techniques. This will mimic the conversion of the substrate protein by infectious PrP. The overall yield and time course of conformational changes in the substrate protein will be determined by monitoring changes in the 7-azatryptophan fluorescence.

The UV absorption and fluorescence emission spectra of W99 α-PrP containing 0% and 90% 7-AzaTrp are displayed in Figure 4. Note the shoulder at 300 nm for 7-AzaTrp; this spectral feature allows the selective excitation of 7-AzaTrp at 310 nm in a background of Trp –containing protein. Excitation with 295 nm light yields large signals for both samples. In contrast, excitation at 310 nm (dashed lines) allow the selective excitation of 7-AzaTrp (7AW), since neither Trp nor Tyr absorb at 310 nm. The sole disadvantage of this method is that the overall fluorescence signals from 7-AzaTrp are relatively small when the samples are excited at 310 nm, owing to the lower absorptivity of the analog at 310 nm compared with 295 nm.

Figure 4. Comparison of the UV and Fluorescence spectra of α-PrP (W99 mutant) with Trp or 7-AzaTrp.
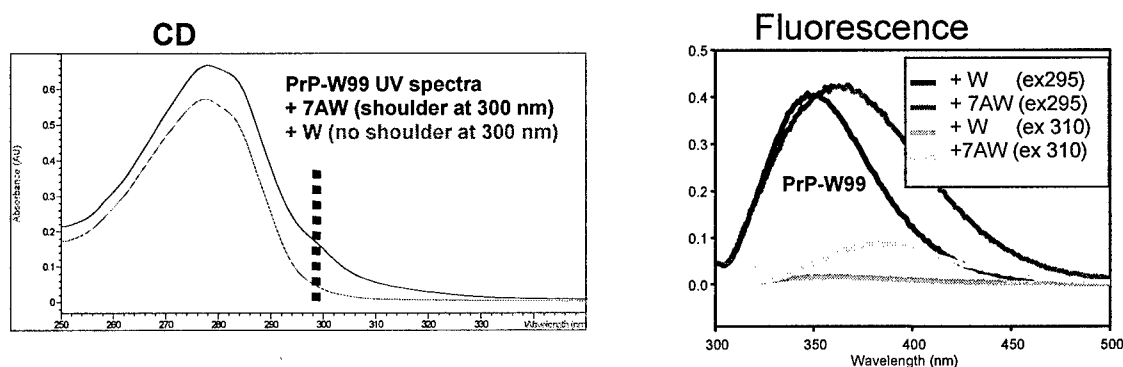
To date, we have examined the fluorescence of 7-AzaTrp in 5 mutants in both the α-PrP and β-PrP forms. Sample spectra are shown in Figure 5 and the data are summarized in Table 5.

Figure 5. Comparison of the fluorescence spectra of α- and β-froms of PrP Y163W mutant containing 7-AzaTrp.

11
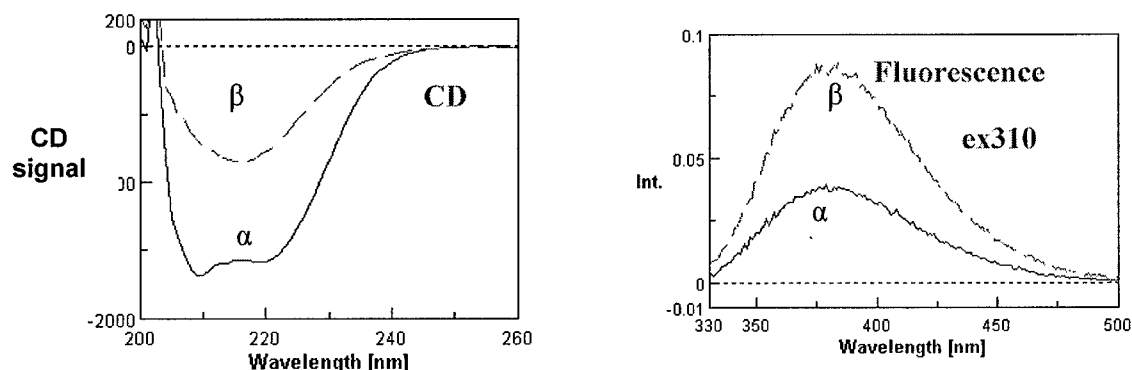
These preliminary data show the utility of 7-AzaTrp incorporation for following structural changes associated with conversion and/or aggregation of PrP. The red-shifted absorbance spectrum of this analog allows it to be selectively excited in the presence of natural Trp and Tyr amino acids. Additionally, the emission spectrum of 7-AzaTrp exhibits large spectral and quantum yield shifts, depending on the polarity and pH of its local environment.

Table 5. Summary of fluorescence data from PrP mutants containing 7-azaTrp.

Protein	α-PrP (λ max, Signal Intensity)		β-PrP (λ max, Signal Intensity)	
W99 (W145Y)	387	0.0401	384	0.0489
W145 (W99F)	384	0.0390	384	0.0408
Y150W (W99F/W145Y)	381	0.0408	381	0.0420
Y163W (W99F/W145Y)	381	0.0369	382	0.0876
Y218W (W99F/W145Y)	381	0.0306	383	0.0489

In these experiments, little change was noted upon conversion, except for mutant Y163W. Moreover, the data are inconsistent with the changes noted for normal Trp. We attribute this to the difference in signal intensity – the spectra were collected on samples of similar concentration, but the relative absorbances at 310 and 295 nm are vastly different. Given the large decrease in absorptivity at 310 nm compared with 295 nm (see Figure 4), we plan to repeat these experiments using higher protein concentrations. Only then will we be able to sensibly interpret the data. These experiments are planned for the coming year, as part of the thesis of Ms. Yanchao Ran. Previously proposed FRET experiments have not been possible, since the time-resolved fluorescence instrumentation is housed in the Spectroscopy Core Facility (Dr. Sandy Ross, director), which has been shut down for the past 8 months due to major construction. The facility should be on-line by September 2005.

KEY RESEARCH ACCOMPLISHMENTS

- Produced, purified, and characterized nine mutants of Syrian hamster prion protein
- Measured the fluorescence emission spectra of these mutants in their normal monomeric α-form
- Determined the fluorescence emission spectra of the nine mutants after conversion to the β-form
- Determined that Y150W is a prime candidate for reporting structural changes that accompany conversion
- Produced prion protein doped with 7-AzaTrp at ~90% incorporation

REPORTABLE OUTCOMES:

Poster Presentation, **Methods in Protein Structural Analysis,** Seattle, WA August 2004. *Probing Prion Protein Conformational Changes by Circular Dichroism and Fluorescence Spectroscopy* *Hui-Chun Yeh* and *Michele A. McGuirl.*

Invited Speaker, The University of Montana - Toyo University Symposium on Bio-Nano Technology and Sciences, September 29-30, 2004. Prion Proteins: Elucidation of the structural changes associated with the diseased state. *Michele McGuirl*

CONCLUSIONS:

We have made substantial progress toward determining key residues of the prion protein that undergo structural perturbations upon conversion to the disease-causing conformation. We have identified several positions that report on the structural changes associated with conversion. We plan to make only a few more mutants that have been chosen based on the two proposed models of β-PrP, the β-spiral and the β-helix. In turn, the fluorescence data will be used to test the validity of these models. The molecular biology should be complete by September 2005. Except for lifetime and FRET measurements, all necessary methodology for future experiments has been developed. We have improved the level of analog incorporation into prion protein, but need to repeat the fluorescence measurements at higher protein concentrations.

In Year 3, we will design a substrate peptide/protein that contains 7-AzaTrp. Through fluorescence changes that occur upon conversion of the substrate by diseased but not normal prion protein, the substrate may be used to detect the presence of disease. The work will also give much needed structural information about the conformational changes that occur upon conversion and may help design drugs to prevent the disease from propagating.

REFERENCES:

1.   B. Caughey *et al., Adv Protein Chem* **57**, 139 (2001).
2.   J. B. Ross, A. G. Szabo, C. W. Hogue, *Methods Enzymol* **278**, 151 (1997).
3.   M.L. DeMarco and V. Daggett, Proc Natl Acad Sci U S A. 101, 2293 (2004).
4.   C. Govaerts, H. Wille, S. B. Prusiner, F. E. Cohen, *Proc Natl Acad Sci U S A.* **101**: 8342 (2004).
5.   E. Paramithiotis *et al., Nat Med* **9**:893 (2003).
6.   T.L. **James, H. Liu, N.B. Ulyanov, S. Farr-Jones, H. Zhang, D.G. Donne, K. Kaneko, D. Groth, I. Mehlhorn, S.B. Prusiner, F.E. Cohen** .*Proc Natl Acad Sci U S A.* **94**:10086 (1997).
7.   B. Holmquist and B.L. Vallee. *Biochemistry.* 12:4409 (1973).
8.   MA McGuirl, CD McCahon, KE McKeown, and DM Dooley. *Plant Physiol.* 106:1205 (1994)
9.   I. V. Baskakov, G. Legname, M. A. Baldwin, S. B. Prusiner, F. E. Cohen, *J Biol Chem* **277**, 21140 (2002).
10.   J. O. Speare, T. S. Rush, 3rd, M. E. Bloom, B. Caughey, *J Biol Chem* **278**, 12522 (2003).
6.   P. Bayley, in *An Introduction to Spectroscopy for Biochemists* S. B. Brown, Ed. (Academic Press, New York, (1980) pp. 148-234.
11.   J. T. Vivian, P. R. Callis, *Biophys J* **80**:2093 (2001).

12. P.R. Callis and T Liu, *J. Phys. Chem. B 108:* 4248 (**2004**)
13. Y Chen and M.D. Barkley *Biochemistry 37:* 9976 (**1998**)

MANUSCRIPTS/REPRINTS, ABSTRACTS
none

APPENDICES

Comparison of the structures of α-PrP (PDB entry 1B10) from (6), β-spiral model from (3), and the β-helix model from (4).

Appendix

Comparison of the α-PrP structure determined by NMR (1B10) with the two proposed models of β-PrP.

Overall structures of:

1A. α-PrP

1B. β-spiral PrP (DeMarco and Daggett).

1C. β-helix PrP (Govaerts , Cohen et al)

The same structures, highlighting the mutation sites investigated in this report in:

2A. α-PrP

2B. β-spiral PrP (DeMarco and Daggett).

2C. β-helix PrP (Govaerts , Cohen et al)

The same structures, ihighlighting the local environment of Y150 in:

3A. α-PrP

3B. β-spiral PrP (DeMarco and Daggett).
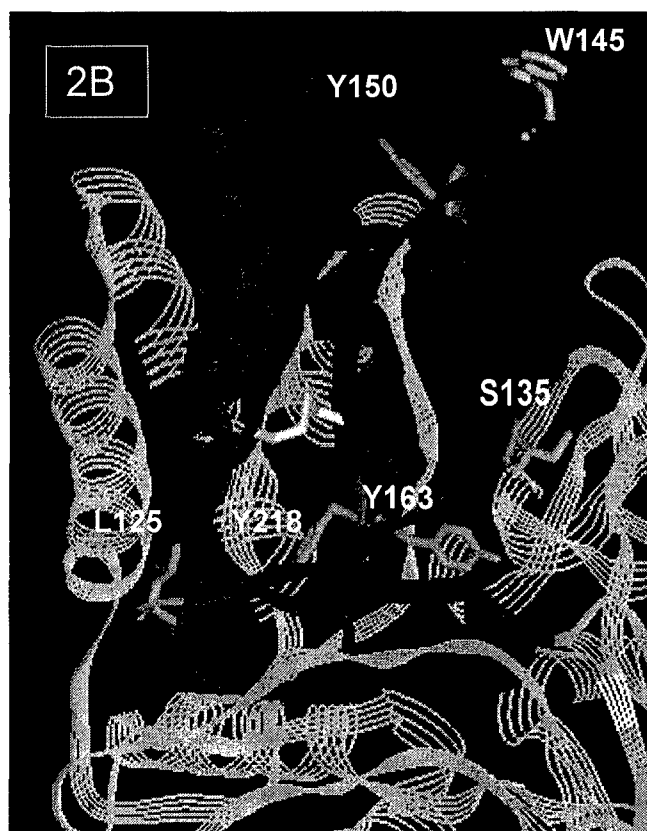
3C. β-helix PrP (Govaerts , Cohen et al)
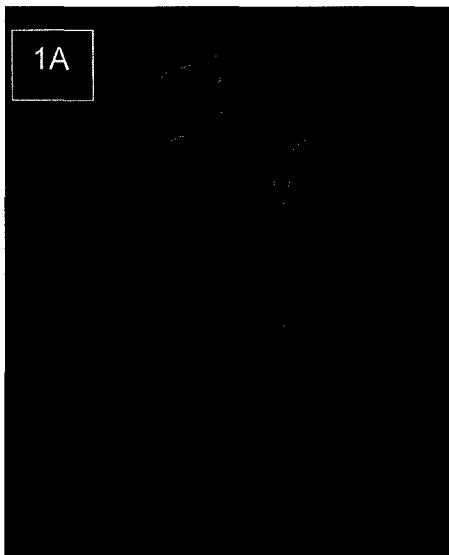
1A. α-PrP monomer, determined by NMR (6).

1B. β-PrP spiral hexameric model from (3). Note there is little rearrangement of the α-helices. A slight increase in β-sheet occurs, creating 3 β-strands on one side of the monomer and 1 on the other. The 3 strands of one monomer interact with the lone strand on another monomer, creating a spiral erstructure that has the potential to form long fibers.

1C. β-PrP helix trimeric model from (4). Note there is substrantial rearrangement of the N-terminus into β-strands. No information is given as to how this trimer might lead to fiber formation
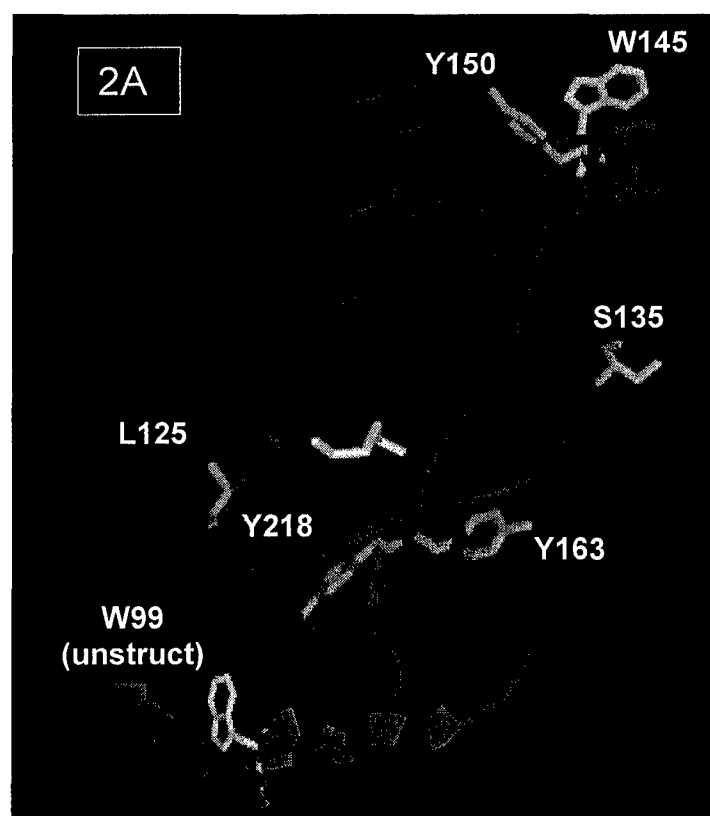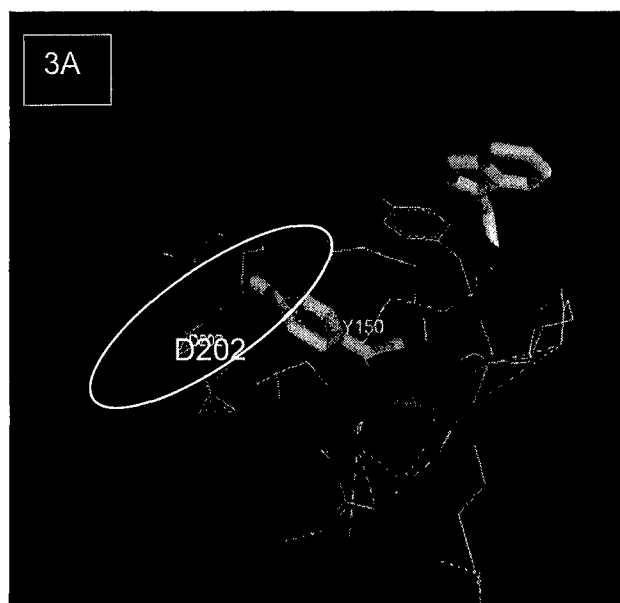
16
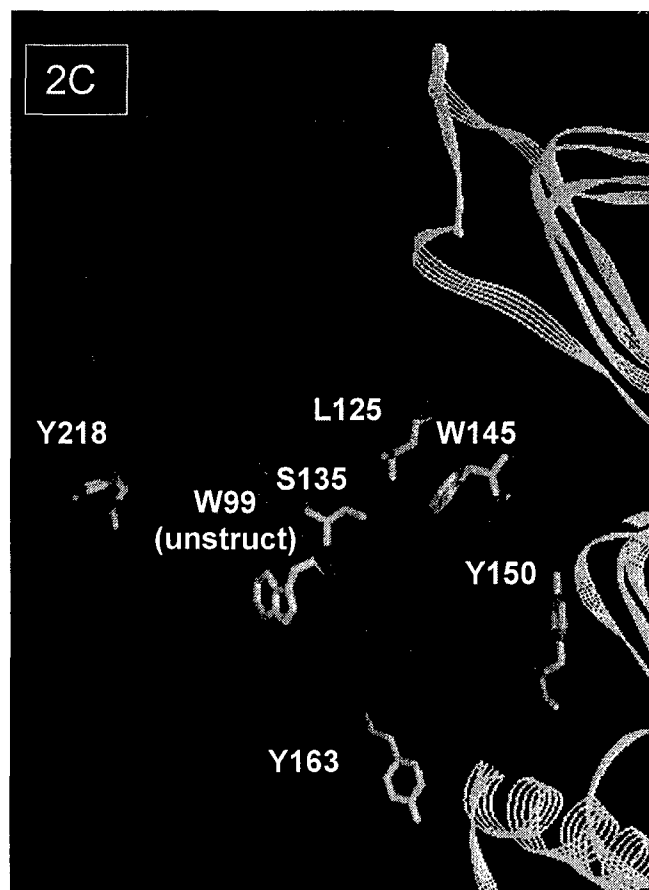
A closeup of the monomers of the same structures, highlighting the mutation sites investigated in this report in:

2A. α-PrP

2B. β-spiral PrP (DeMarco and Daggett).

2C. β-helix PrP (Govaerts , Cohen et al)

3A

3B

3C

A closeup of Y150 in the same structures

3A. α-PrP. H bonding to D202 is shown.

3B. β-spiral PrP (DeMarco and Daggett). No H bond is predicted.

3C. β-helix PrP (Govaerts , Cohen et al). Closeness of H110 and Arg148 ar shown. Residues of the second subunit are in pink.

18